



Published in final edited form as:

J Hand Surg Am. 2013 February ; 38(2): 241–249. doi:10.1016/j.jhsa.2012.11.007.

Biomechanical Contributions of Posterior Deltoid and Teres Minor in the Context of Axillary Nerve Injury: A Computational Study

Dustin L. Crouch, BS^{1,2}, Johannes F. Plate, MD^{3,4}, Zhongyu Li, MD, PhD³, and Katherine R. Saul, PhD^{1,2}

¹Virginia Tech-Wake Forest School of Biomedical Engineering and Sciences, Winston-Salem, NC, 27157

²Department of Biomedical Engineering, Wake Forest School of Medicine, Winston-Salem, NC, 27157

³Department of Orthopaedic Surgery, Wake Forest School of Medicine, Winston-Salem, NC, 27157

⁴Neuroscience Program, Wake Forest School of Medicine, Winston-Salem, NC, 27157

Abstract

Purpose—To determine if transfer to only the anterior branch of the axillary nerve will restore useful function following axillary nerve injury with persistent posterior deltoid and teres minor paralysis.

Methods—We used a computational musculoskeletal model of the upper limb to determine the relative contributions of posterior deltoid and teres minor to maximum joint moment generated during a simulated static strength assessment and to joint moments during 3 sub-maximal shoulder movements. Movement simulations were performed with and without simulated posterior deltoid and teres minor paralysis to identify muscles which may compensate for their paralysis.

Results—In the unimpaired limb model, teres minor and posterior deltoid accounted for 16% and 14% of the total isometric shoulder extension and external rotation joint moments, respectively. During the 3 movement simulations, posterior deltoid produced as much as 20% of the mean shoulder extension moment, while teres minor accounted for less than 5% of the mean joint moment in all directions of movement. When posterior deltoid and teres minor were paralyzed, the mean extension moments generated by the supraspinatus, long head of triceps, latissimus dorsi, and middle deltoid increased to compensate. Compensatory muscles were not fully activated during movement simulations when posterior deltoid and teres minor were paralyzed.

Conclusions—Reconstruction of the anterior branch of the axillary nerve only is an appropriate technique for restoring shoulder abduction strength following isolated axillary nerve injury. When shoulder extension strength is compromised by extensive neuromuscular shoulder injury,

© 2012 The American Society for Surgery of the Hand. Published by Elsevier Inc. All rights reserved.

Corresponding Author: Dustin L. Crouch, BS, Address: Wake Forest Baptist Health, Mailstop 573511, Medical Center Boulevard, Winston-Salem, NC 27157, dcrouch@wfubmc.edu, Phone: 336-713-1450, Fax: 336-716-5491.

Publisher's Disclaimer: This is a PDF file of an unedited manuscript that has been accepted for publication. As a service to our customers we are providing this early version of the manuscript. The manuscript will undergo copyediting, typesetting, and review of the resulting proof before it is published in its final citable form. Please note that during the production process errors may be discovered which could affect the content, and all legal disclaimers that apply to the journal pertain.

reconstruction of both the anterior and posterior branches of the axillary nerve should be considered.

Clinical Relevance—By quantifying the biomechanical role of muscles during sub-maximal movement, in addition to quantifying muscle contributions to maximal shoulder strength, we can inform pre-operative planning and permit more accurate predictions of functional outcomes.

Keywords

biomechanics; deltoid; nerve; shoulder; simulation

Introduction

The axillary nerve is the most commonly injured nerve following shoulder trauma (1, 2). Axillary nerve injuries after shoulder surgical procedures have also been well-recognized (3, 4). When watchful observation and therapy fail to improve deltoid function, surgical axillary nerve repair may be necessary to restore shoulder abduction strength required for activities of daily living. The axillary nerve's anterior branch innervates the anterior and middle deltoid, while its posterior branch innervates posterior deltoid and teres minor (4, 5). Nerve grafting, traditionally the preferred surgical treatment for isolated axillary nerve lesions, potentially restores both axillary nerve branches (6). Nerve transfer to the anterior branch of the axillary nerve has been recognized as a possible alternative to nerve grafting, despite persistent posterior deltoid and teres minor paralysis following nerve transfer (7).

The effect of teres minor and posterior deltoid paralysis on functional outcomes following nerve transfer depends in part on each muscle's contribution to maximum joint moment, a common measure of strength (8, 9). Previous biomechanical studies have evaluated the maximum joint moments generated by maximally-activated muscles crossing the shoulder during isokinetic movements (10, 11). Anatomical properties such as muscle path (as measured by moment arm) (12–14) and muscle cross-sectional area (10) have also been used to calculate the potential maximal strength of individual muscles crossing the shoulder. However, muscles crossing the shoulder are often sub-maximally and unequally activated during daily living tasks, so each muscles' relative contributions to the performance of such tasks may differ from their contributions to maximum joint strength (15, 16). Additionally, when the posterior deltoid and teres minor are paralyzed, joint moments produced by non-paralyzed muscles may change to compensate (17).

The joint moment generated by a muscle is determined by its maximum strength (a function of length, cross-sectional area, and moment arm) and its state of activation, which are difficult to measure experimentally in vivo. Computational musculoskeletal models implemented for dynamic movement simulation incorporate numerous experimentally-determined muscle properties that allow predictions of muscle activations and joint moments produced during daily living tasks. Dynamic simulation has been used with upper limb models to evaluate the biomechanics of wheelchair propulsion (18) and to predict pinch forces following brachioradialis tendon transfer (19).

The objective of this study was to determine whether the posterior branch of the axillary nerve should be reconstructed based on the biomechanical roles of the posterior deltoid and teres minor in shoulder strength and movement ability. We evaluated the relative contributions of posterior deltoid and teres minor to maximum joint moments generated during a simulated static strength assessment and to joint moments produced during dynamic simulations of 3 sub-maximal shoulder movements both with and without simulated paralysis of the posterior deltoid and teres minor. Muscles which generated greater joint moments to compensate for posterior deltoid and teres minor paralysis were

identified. We hypothesized that the posterior deltoid and teres minor would contribute little to maximum shoulder strength and to joint moments during sub-maximal movement.

Materials and Methods

We used a 3-dimensional computer model of the upper limb musculoskeletal system (20) implemented for dynamic movement simulation (21) in the OpenSim 2.4 modeling and simulation software (Stanford University, CA) (22). The model has been widely used and validated for simulation of healthy and impaired upper limb orthopedic conditions (18, 23–27). We used a simplified model that included the architecture and origin-to-insertion paths of 32 muscles and muscle compartments crossing the shoulder and elbow and included movement of the shoulder and shoulder girdle, elbow flexion, and forearm rotation (24). Upper limb anthropometry represented a 50th percentile adult male. Maximum forces that the muscles could produce were based on strength and muscle volume measurements from young, healthy, adult male subjects (28, 29). Muscles crossing the glenohumeral joint included the deltoid, supraspinatus, infraspinatus, subscapularis, teres minor, teres major, pectoralis major, latissimus dorsi, coracobrachialis, the long head of triceps, and the long and short heads of biceps.

We first determined the maximum strength of teres minor and the 3 deltoid compartments (anterior, middle, posterior) relative to all muscles crossing the shoulder during a simulated strength assessment with the upper limb in a fixed, static posture (Figure 1). This simulated static strength assessment is analogous to clinical strength assessments performed with a dynamometer (8). Second, we used the model to simulate abduction, shoulder extension, and external rotation movements to determine how the teres minor and the 3 deltoid compartments contribute to sub-maximal shoulder movements (Figure 2). These 3 movements are commonly assessed clinically as a measure of functional recovery following nerve transfer at the shoulder (6, 30) and are important components of more complex movements such as touching the face or reaching. The 3 movements were simulated using models that represented either an unimpaired limb or an impaired limb with isolated posterior deltoid and teres minor paralysis, based on procedures reconstructing the anterior branch of the axillary nerve only following axillary nerve injury (7). We compared computed joint moments and muscle activations between movement simulations with the unimpaired and impaired limb model to identify possible neuromuscular compensation strategies for posterior deltoid and teres minor paralysis.

Simulated maximum isometric shoulder strength assessment

We calculated the maximum isometric joint moment that each individual muscle crossing the shoulder could generate in 6 possible directions of shoulder movement: abduction, adduction, internal axial rotation, external axial rotation, shoulder flexion, and shoulder extension. The maximum isometric joint moment a muscle could generate was a function of several musculoskeletal anatomical properties, including muscle physiological cross-sectional area, muscle fiber length, muscle-tendon length, and moment arm. All maximum isometric joint moments were calculated in the same static, fixed shoulder posture, in which the arm was at 45° of elevation in the coronal plane, with the elbow in full extension, and the forearm in neutral pronation/supination (Figure 1).

Simulated sub-maximal movements

Simulations of 3 simple shoulder movements were performed (Figure 2). Shoulder joint angles were referenced from a neutral posture of full arm adduction, full elbow extension, and neutral forearm pronation/supination; and the movements were synthetically generated to move the shoulder smoothly in 1 degree of freedom for each movement. Unless otherwise

stated, all joints were in a neutral posture during the movement simulations. During the abduction simulation, the arm was elevated from 0° to 90° in the coronal plane over 3 seconds. During the shoulder extension simulation, the shoulder was extended from 45° shoulder flexion to 10° shoulder extension over 2 seconds against a 5 lb (22 N) resistance applied at the hand, while the arm was held at 20° elevation from the sagittal plane. The elbow flexion angle varied during the simulation to maintain the forearm parallel to the axial plane. External rotation was simulated from 20° internal rotation to 10° external rotation over 1 second against a 5 lb (22 N) resistance applied at the hand, with the elbow at 90° flexion.

A computational method, computed muscle control, was used to predict the muscle activations and forces required to simulate the 3 movements (31). Because more muscles cross the upper limb joints than are required to rotate the joints during movement, we use this method which assumes that muscles are coordinated such that the total metabolic effort exerted by all muscles is minimized during the movement. Muscle activations calculated during computed muscle control ranged from 0 (inactivated) to 1 (fully activated). Active force generated by each muscle was a function of its state of activation, maximum force generating potential, length, and rate of change of length. The total force generated by each muscle was the sum of active and passive forces produced by the muscle. Co-contraction of opposing muscles was permitted if it was necessary to perform the desired movement while minimizing the total metabolic effort.

We calculated the mean joint moment each muscle crossing the shoulder produced during the 3 movement simulations. Muscles could potentially generate joint moment in 6 possible directions of shoulder movement: abduction, adduction, internal axial rotation, external axial rotation, shoulder flexion, and shoulder extension. Joint moments generated during movement accounted for each muscle's moment-generating potential (determined from muscle cross section, length, and moment arm) and state of activation during the movement.

Results

Simulated maximum isometric shoulder strength assessment

Both the teres minor and posterior deltoid generated a combined 16% of the total maximum isometric shoulder extension moment and 14% of the total maximum isometric external rotation moment (Figure 3). The combined contribution of these muscles to total isometric abduction and adduction joint moment was 4% and 3%, respectively. By comparison, middle deltoid accounted for 58% of the total maximum isometric abduction moment, while anterior deltoid accounted for 37% of the total maximum isometric shoulder flexion moment.

Unimpaired sub-maximal movement simulations

The teres minor and posterior deltoid primarily generated shoulder extension and external rotation joint moments (Figure 4). Posterior deltoid produced 20% and 11% of the total mean shoulder extension moment during the abduction and shoulder extension simulations, respectively. During the external rotation simulation, the teres minor accounted for 5% of the total mean adduction moment, more than in any other direction of movement during the 3 simulations. Middle deltoid accounted for 59% to 73% of the total mean abduction moment during the 3 movement simulations. Anterior deltoid produced 34% and 55% of the total mean shoulder flexion moment during the abduction and shoulder extension simulations, respectively.

Compensation for muscle paralysis during sub-maximal movement simulations

Because the posterior deltoid primarily contributed to shoulder extension moments during movements, other muscles crossing the shoulder compensated for posterior deltoid paralysis by generating greater shoulder extension joint moments. During the abduction simulation, the mean extension moments generated by the supraspinatus, long head of triceps, and latissimus dorsi were 44%, 52%, and 38% higher, respectively, when the posterior deltoid and teres minor were paralyzed (Figure 5). Likewise, during the extension simulation, the mean shoulder extension moments generated by the middle deltoid, long head of triceps, and latissimus dorsi were 6%, 16%, and 19% higher, respectively, when the posterior deltoid and teres minor were paralyzed.

Muscles that generated greater mean shoulder extension moments to compensate for posterior deltoid and teres minor paralysis also exhibited increased mean and maximum muscle activations (Figure 6). Supraspinatus mean and maximum activations increased the most of any other compensatory muscle during the 3 movement simulations. During the abduction simulation, the mean activation of the supraspinatus increased from 0.28 to 0.38 when the posterior deltoid and teres minor were paralyzed, while its maximum activation increased from 0.61 to 0.86. During the shoulder extension simulation, the mean activation of the long head of triceps increased from 0.13 to 0.17, and its maximum activation increased from 0.49 to 0.63, when the posterior deltoid and teres minor were paralyzed. Compensatory muscles were not maximally activated during the simulations, even when the posterior deltoid and teres minor were paralyzed.

Discussion

Anterior and middle deltoid were greater contributors to maximum isometric shoulder strength and to joint moments generated during sub-maximal movements than the posterior deltoid and teres minor. During the simulated maximum strength assessment, the middle deltoid accounted for 58% of the total maximum isometric abduction strength, compared to only 4% by the posterior deltoid. During the movement simulations, the anterior and middle deltoid accounted for 34% to 73% of the total mean abduction and shoulder flexion joint moments, while the posterior deltoid produced no more than 20% of the total mean joint moment in any direction of shoulder movement.

The model had sufficient strength to simulate the 3 movements even when the posterior deltoid and teres minor were paralyzed. Muscles that compensated for posterior deltoid paralysis by generating greater shoulder extension moments included the supraspinatus, long head of triceps, latissimus dorsi, and middle deltoid. Muscle activations of the supraspinatus and the long head of triceps increased the most of all compensatory muscles. However, compensatory muscles were not fully activated during the movement simulations, indicating that the shoulder musculature had sufficient residual strength to accommodate additional shoulder weakness or perform tasks demanding greater strength.

Our simulation results suggest that reconstructing only the anterior branch of the axillary nerve is an acceptable technique for restoring shoulder function following isolated axillary nerve injury. Reconstruction procedures limited to the anterior branch of the axillary nerve have achieved good recovery of abduction strength despite persistent paralysis of the posterior deltoid and teres minor (7). Anterior and middle deltoid recovery may even be superior when reconstruction is limited to the anterior axillary branch, as more donor nerve fibers are available to reinnervate the targeted muscles (7).

It may be advantageous to restore innervations to the posterior deltoid and teres minor when neuromuscular shoulder injury is not limited to the axillary nerve. The posterior deltoid

contributes to shoulder extension, which is required to perform certain functional tasks, including perineal care and touching the back of the head (32, 33). Concomitant neuromuscular injuries may limit the ability of the supraspinatus, long head of triceps, and other muscles crossing the shoulder to biomechanically compensate for posterior deltoid paralysis. For example, shoulder dislocation may cause both an axillary nerve injury and a supraspinatus tear (4, 34). Humerus fractures can cause radial nerve palsy and paralysis of the long head of triceps (35). Brachial plexus injury involving the C5 and C6 nerve roots paralyzes several muscles that generate shoulder extension moments, including the posterior deltoid, teres minor, supraspinatus, and infraspinatus (12, 36). In such cases, reconstruction of both posterior and anterior branches of the axillary nerve should be considered.

Previous studies investigating deltoid strength and activity during movement fail to quantify its contribution to joint moments generated during sub-maximal daily living tasks. In subjects receiving alternating axillary and suprascapular nerve block, the deltoid accounted for approximately 50% of the total maximum isokinetic forward flexion and scapular abduction moment (10). By comparison, our computational model predicted that the deltoid accounts for 62% of the total maximum isometric abduction moment at 45 degrees of shoulder elevation. Experimental moment arm measurements confirm that the posterior deltoid can generate extension moments in several postures (12). Electromyographic recordings show that the anterior and middle deltoid exhibit high activation levels during abduction, while the posterior deltoid exhibits low activation (15). This pattern of deltoid compartment activation is consistent with muscle activations calculated during our abduction simulations. The teres minor contributes to external rotation and adduction joint moments based on its moment arm (14), consistent with our results.

We evaluated 2 hypothetical, simplified clinical conditions of axillary nerve transfer following isolated axillary nerve injury, either with or without persistent paralysis of the posterior deltoid and teres minor, to identify the largest possible biomechanical contributions of these muscles. However, we did not simulate other clinical factors associated with axillary nerve injury and reconstruction that can affect neuromuscular function. For example, muscles of donor nerve branches are paralyzed during the axillary nerve transfer procedure (37). Incomplete strength recovery following nerve reconstruction lends to residual weakness in restored muscles (6, 38). Axillary nerve injury can occur in isolation, but other concomitant neuromuscular shoulder injuries following shoulder trauma are common (4, 34–36). Therefore, the results of this study should be considered in the context of each patient's complete clinical condition and used to guide the choice of repair strategy in light of other affected muscles.

We assumed that scapular kinematics were unaffected by nerve injury. However, scapular motion may be compromised following nerve injury involving muscles crossing the shoulder (39, 40). This study highlights the contributions of the posterior deltoid and teres minor to strength and movement about the glenohumeral joint, which these muscles cross. In future studies, the role of the deltoid and teres minor in scapular motion and the effect of residual weakness or paralysis of these muscles on neuromuscular control of shoulder girdle movement must be explored.

We used a mathematical algorithm to predict muscle activations that minimize metabolic effort during the simulated movements. Muscle activations predicted with the computed muscle control algorithm have demonstrated consistency with measured electromyograms during movement in both the upper and lower limb (21, 22, 27, 31). However, patients following nerve transfer may adopt muscle coordination patterns and compensation strategies that do not optimize metabolic effort. Electromyographic recording techniques for predicting activation levels during movement in healthy subjects (15) may generate more

physiologic estimates of motor control patterns during shoulder movement in patients with neuromuscular injury. Muscle activations computed from movement simulations can form the basis of hypotheses about impaired muscle coordination strategies that can be tested experimentally in future studies.

As treatments to restore muscle function following nerve injury become more effective, the biomechanical role of restored muscles has a greater influence on treatment outcomes. Our simulation approach allowed us to evaluate the biomechanical effect of choosing or declining to restore the posterior branch of the axillary nerve apart from other clinical and subject-specific factors that affect functional outcome. Understanding the individual muscle contributions to strength and movement ability at the shoulder can inform preoperative planning and permit more accurate predictions of functional outcomes.

Acknowledgments

This work was supported by the National Institutes of Health (NIH 5R24HD050821-02) and the Wake Forest School of Medicine.

References

1. Payne MW, Doherty TJ, Sequeira KA, Miller TA. Peripheral nerve injury associated with shoulder trauma: a retrospective study and review of the literature. *J Clin Neuromuscul Dis.* 2002; 4(1):1–6. [PubMed: 19078679]
2. Perlmutter GS. Axillary nerve injury. *Clin Orthop Relat Res.* 1999; (368):28–36. [PubMed: 10613150]
3. Zhang J, Moore AE, Stringer MD. Iatrogenic upper limb nerve injuries: a systematic review. *ANZ J Surg.* 2011; 81(4):227–236. [PubMed: 21418465]
4. Apaydin N, Tubbs RS, Loukas M, Duparc F. Review of the surgical anatomy of the axillary nerve and the anatomic basis of its iatrogenic and traumatic injury. *Surg Radiol Anat.* 2010; 32(3):193–201. [PubMed: 19916067]
5. Uz A, Apaydin N, Bozkurt M, Elhan A. The anatomic branch pattern of the axillary nerve. *J Shoulder Elbow Surg.* 2007; 16(2):240–244. [PubMed: 17097311]
6. Okazaki M, Al-Shawi A, Gschwind CR, Warwick DJ, Tonkin MA. Outcome of axillary nerve injuries treated with nerve grafts. *J Hand Surg Eur Vol.* 2011; 36(7):535–540. [PubMed: 21546415]
7. Leechavengvongs S, Witoonchart K, Uerpairojkit C, Thuvasethakul P. Nerve Transfer to Deltoid Muscle Using the Nerve to the Long Head of the Triceps, Part II: A Report of 7 Cases. *J Hand Surg.* 2003; 28A(4):633–638.
8. Kim HM, Teefey SA, Zelig A, Galatz LM, Keener JD, Yamaguchi K. Shoulder strength in asymptomatic individuals with intact compared with torn rotator cuffs. *J Bone Joint Surg Am.* 2009; 91(2):289–296. [PubMed: 19181972]
9. Vidt ME, Daly M, Miller ME, Davis CC, Marsh AP, Saul KR. Characterizing upper limb muscle volume and strength in older adults: a comparison with young adults. *J Biomech.* 2012; 45(2):334–341. [PubMed: 22047782]
10. Howell SM, Imobersteg AM, Seger DH, Marone PJ. Clarification of the Role of the Supraspinatus Muscle in Shoulder Function. *J Bone Joint Surg Am.* 1986; 68A(3):398–404. [PubMed: 3949834]
11. David G, Magarey ME, Jones MA, Dvir Z, Turker KS, Sharpe M. EMG and strength correlates of selected shoulder muscles during rotations of the glenohumeral joint. *Clin Biomech.* 2000; 15(2): 95–102.
12. Kuechle DK, Newman SR, Morrey BF, An K-N. Shoulder muscle moment arms during horizontal flexion and elevation. *J Shoulder Elb Surg.* 1997; 6(5):429–439.
13. Liu J, Hughes RE, Smutz WP, Niebur G, Nan-An K. Roles of deltoid and rotator cuff muscles in shoulder elevation. *Clin Biomech.* 1997; 12:32–38.

14. Otis JC, Jiang CC, Wickiewicz TL, Peterson MG, Warren RF, Santner TJ. Changes in the moment arms of the rotator cuff and deltoid muscles with abduction and rotation. *J Bone Joint Surg Am.* 1994; 76:667–676. [PubMed: 8175814]
15. Wickham J, Pizzari T, Stansfeld K, Burnside A, Watson L. Quantifying ‘normal’ shoulder muscle activity during abduction. *J Electromyography Kinesiol.* 2010; 20:212–222.
16. Kronberg M, Nemeth G, Brostrom LA. Muscle activity and coordination in the normal shoulder. An electromyographic study. *Clin Orthop Relat Res.* 1990; 257:76–85. [PubMed: 2379377]
17. McCully SP, Suprak DN, Kosek P, Karduna AR. Suprascapular nerve block results in a compensatory increase in deltoid muscle activity. *J Biomech.* 2007; 40:1839–1846. [PubMed: 17034796]
18. Rankin JW, Kwarcia AM, Richter WM, Neptune RR. The influence of altering push force effectiveness on upper extremity demand during wheelchair propulsion. *J Biomech.* 2010; 43(14): 2771–2779. [PubMed: 20674921]
19. Mogk JPM, Johanson ME, Hentz VR, Saul KR, Murray WM. A simulation analysis of the combined effects of muscle strength and surgical tensioning on lateral pinch force following brachioradialis to flexor pollicis longus transfer. *J Biomech.* 2011; 44(4):669–675. [PubMed: 21092963]
20. Holzbaur KRS, Murray WM, Delp SL. A Model of the Upper Extremity for Simulating Musculoskeletal Surgery and Analyzing Neuromuscular Control. *Ann Biomed Eng.* 2005; 33(6): 829–840. [PubMed: 16078622]
21. Daly, M. Adaptations following upper extremity resistance training in older adults. Winston-Salem, NC: School of Biomedical Engineering Sciences, Wake Forest University Graduate School of Arts and Sciences; 2011.
22. Delp SL, Anderson FC, Arnold AS, et al. OpenSim: Open-Source Software to Create and Analyze Dynamic Simulations of Movement. *IEEE Trans Biomed Eng.* 2007; 54(11):1940–1950. [PubMed: 18018689]
23. Saul KR, Murray WM, Hentz VR, Delp SL. Biomechanics of the Steindler Flexorplasty Surgery: A Computer Simulation Study. *J Hand Surg.* 2003; 28A(6):979–986.
24. Crouch DL, Li Z, Barnwell J, Plate JF, Daly M, Saul KR. Computer simulation of nerve transfer strategies for restoring shoulder function after adult C5 and C6 root avulsion injuries. *J Hand Surg Am.* 2011; 36(10):1644–1651. [PubMed: 21903345]
25. Saul KR, Hayon S, Smith TL, Tuohy CJ, Mannava S. Postural dependence of passive tension in the supraspinatus following rotator cuff repair: a simulation analysis. *Clin Biomech (Bristol, Avon).* 2011; 26(8):804–810.
26. Rankin JW, Richter WM, Neptune RR. Individual muscle contributions to push and recovery subtasks during wheelchair propulsion. *J Biomech.* 2011; 44(7):1246–1252. [PubMed: 21397232]
27. Vandenberghe A, Bosmans L, De Schutter J, Swinnen S, Jonkers I. Quantifying individual muscle contribution to three-dimensional reaching tasks. *Gait Posture.* 2012; 35(4):579–584. [PubMed: 22410130]
28. Holzbaur KRS, Delp SL, Gold GE, Murray WM. Moment-generating capacity of upper limb muscles in healthy adults. *J Biomech.* 2007; 40:2442–2449. [PubMed: 17250841]
29. Holzbaur KRS, Murray WM, Gold GE, Delp SL. Upper limb muscle volumes in adult subjects. *J Biomech.* 2007; 40:742–749. [PubMed: 17241636]
30. Leechavengvongs S, Witoonchart K, Uerpaiojkit C, Thuvasethakul P, Malungpaishrope K. Combined nerve transfers for C5 and C6 brachial plexus avulsion injury. *J Hand Surg Am.* 2006; 31A(2):183–189. [PubMed: 16473676]
31. Leechavengvongs S, Witoonchart K, Uerpaiojkit C, Thuvasethakul P. Nerve Transfer to Deltoid Muscle Using the Nerve to the Long Head of the Triceps, Part II: A Report of 7 Cases. *J Hand Surg.* 2003; 28A(4):633–638.
32. Thelen DG, Anderson FC. Using computed muscle control to generate forward dynamic simulations of human walking from experimental data. *J Biomech.* 2006; 39:1107–1115. [PubMed: 16023125]
33. Andel, CJv; Wolterbeek, N.; Doorenbosch, CAM.; Veeger, D.; Harlaar, J. Complete 3D kinematics of upper extremity functional tasks. *Gait Posture.* 2008; 27:120–127. [PubMed: 17459709]

34. Magermans DG, Chadwick EKJ, Veeger HEJ, Helm FCTvd. Requirements for upper extremity motions during activities of daily living. *Clin Biomech*. 2005; 20:591–599.
35. Berbig R, Weishaupt D, Prim J, Shahin O. Primary anterior shoulder dislocation and rotator cuff tears. *J Shoulder Elbow Surg*. 1999; 8(3):220–225. [PubMed: 10389076]
36. Kettelkamp DB, Alexander H. Clinical review of radial nerve injury. *J Trauma*. 1967; 7(3):424–432. [PubMed: 6024140]
37. Bertelli JA, Ghizoni MF. Reconstruction of C5 and C6 Brachial Plexus Avulsion Injury by Multiple Nerve Transfers: Spinal Accessory to Suprascapular, Ulnar Fascicles to Biceps Branch, and Triceps Long or Lateral Head Branch to Axillary Nerve. *J Hand Surg*. 2004; 29A(1):131–139.
38. Terzis JK, Barmptsioti A. Axillary Nerve Reconstruction in 176 Posttraumatic Plexopathy Patients. *Plast Reconstr Surg*. 2009; 125:233–247. [PubMed: 20048615]
39. Krishnan KG, Martin KD, Schackert G. Traumatic Lesions of the Brachial Plexus: An Analysis of Outcomes in Primary Brachial Plexus Reconstruction and Secondary Functional Arm Reanimation. *Neurosurg*. 2008; 62(4)
40. Dayanidhi S, Orlin M, Kozin S, Duff S, Karduna A. Scapular kinematics during humeral elevation in adults and children. *Clin Biomech (Bristol, Avon)*. 2005; 20(6):600–606.
41. Duff SV, Dayanidhi S, Kozin SH. Asymmetrical shoulder kinematics in children with brachial plexus birth palsy. *Clin Biomech (Bristol, Avon)*. 2007; 22(6):630–638.

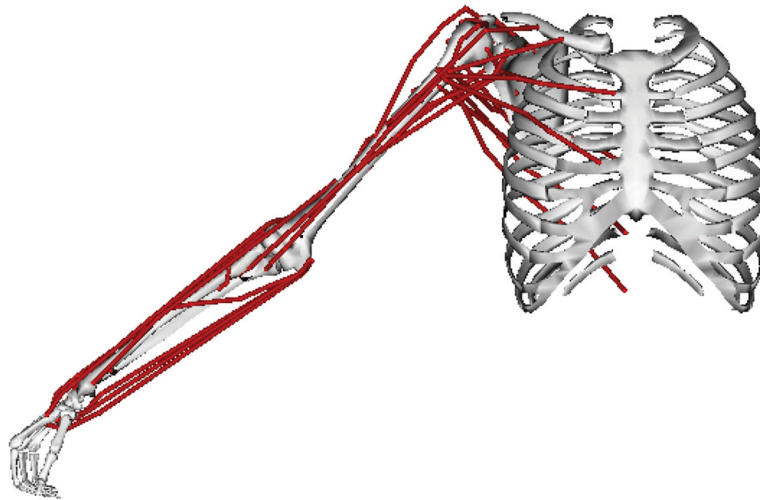


Figure 1. Static posture in which the simulated strength assessment was performed
The arm was at 45° of shoulder elevation in the coronal plane with the elbow, forearm, and wrist in neutral positions.

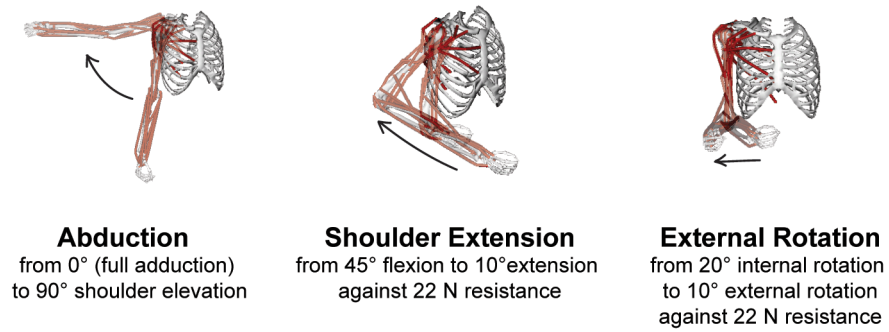


Figure 2. Three movements simulated in the computational upper limb musculoskeletal model
The model is shown in the beginning and end postures, and the direction of each movement is indicated by an arrow.

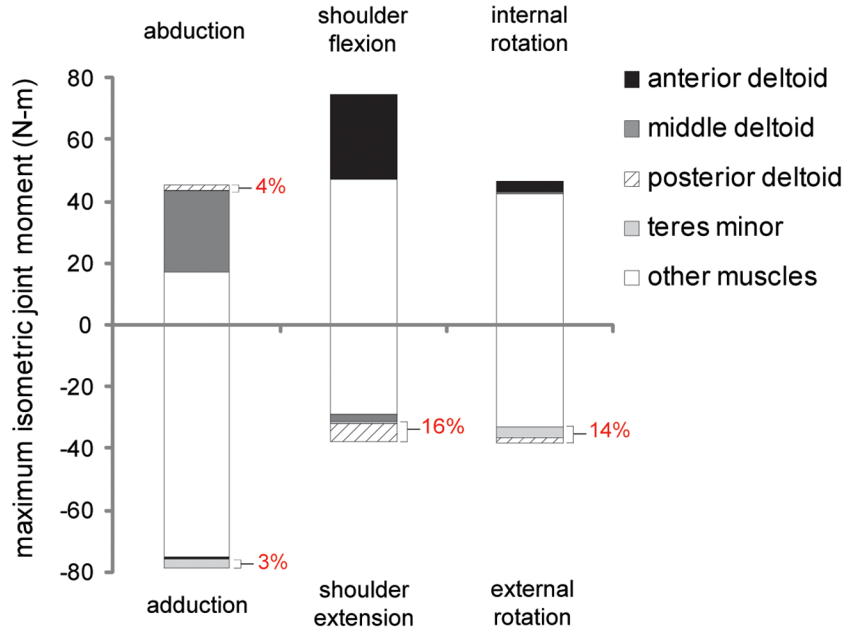


Figure 3. Maximum isometric joint moments produced by muscles crossing the shoulder during a simulated static strength assessment

Joint moments were calculated with the arm at 45° of shoulder elevation in the coronal plane, and the elbow, forearm, and wrist in neutral positions. Maximum isometric joint moments were computed in 6 possible directions of shoulder movement. Positive joint moments were generated in the direction of abduction, shoulder flexion, and internal rotation. Negative joint moments were generated in the direction of adduction, shoulder extension, and external rotation. For each direction of shoulder movement, the combined maximum isometric joint moments of both the posterior deltoid and teres minor as a percentage of the total maximum isometric joint moment are indicated on the figure.

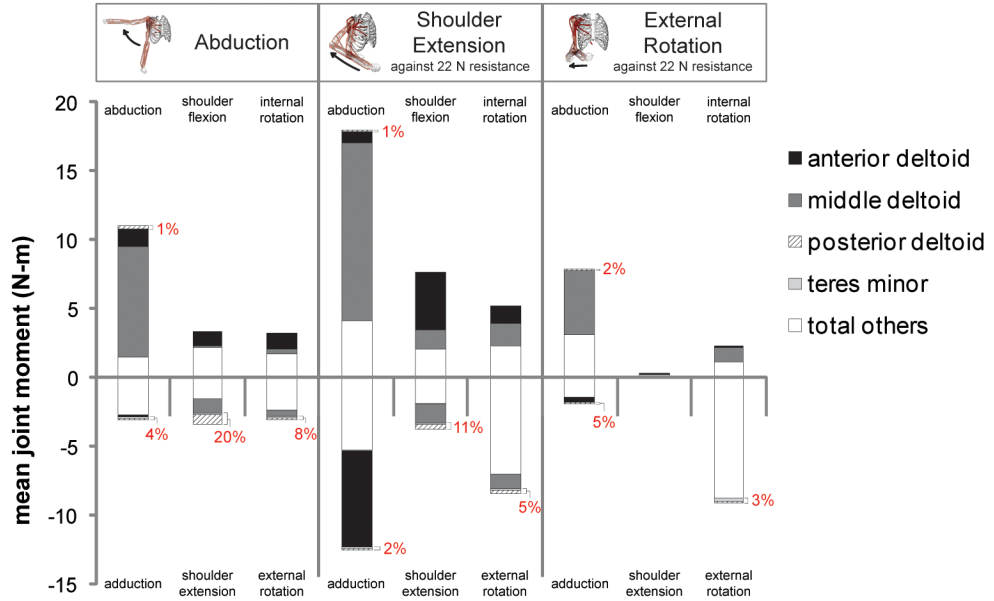


Figure 4. Mean joint moments generated by muscles crossing the shoulder during simulated abduction, shoulder extension, and external rotation movements

The 3 simulated movements are labeled at the top of the figure. Mean joint moments were computed in 6 possible directions of shoulder movement, which are labeled for each simulated movement. Positive joint moments were generated in the direction of abduction, shoulder flexion, and internal rotation. Negative joint moments were generated in the direction of adduction, shoulder extension, and external rotation. Some muscles generated joint moments in both agonist and antagonist directions (e.g. abduction and adduction), indicating that their moment arms changed direction during the simulations. For each direction of shoulder movement, the combined mean joint moments of both the posterior deltoid and teres minor as a percentage of the total mean joint moment are indicated on the figure. The posterior deltoid contributed to abduction, adduction, shoulder extension, and external rotation joint moments, and the teres minor contributed to adduction, shoulder extension, and external rotation joint moments.

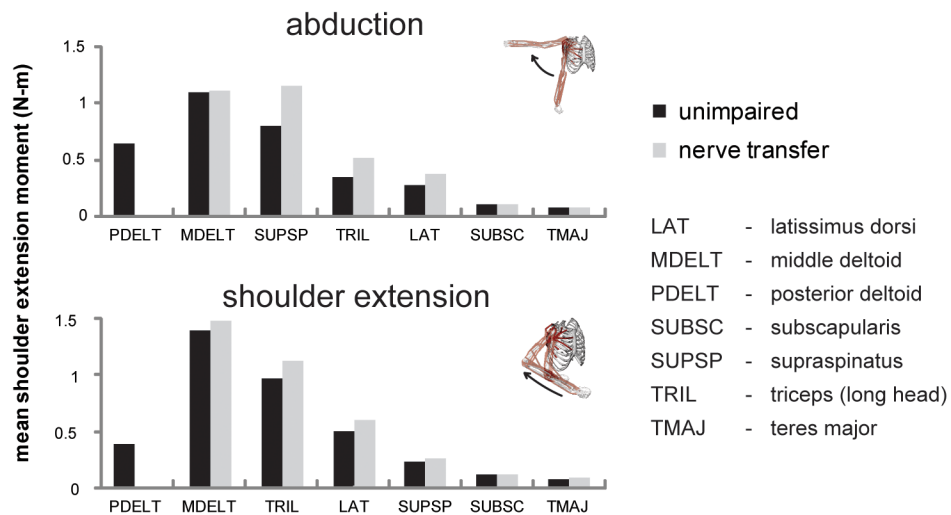


Figure 5. Mean joint moments generated in the direction of shoulder extension by muscles crossing the shoulder during the abduction and shoulder extension movement simulations, both with and without simulated posterior deltoid and teres minor paralysis

The supraspinatus, long head of triceps, latissimus dorsi, and middle deltoid generated greater extension moments when the posterior deltoid and teres minor were paralyzed.

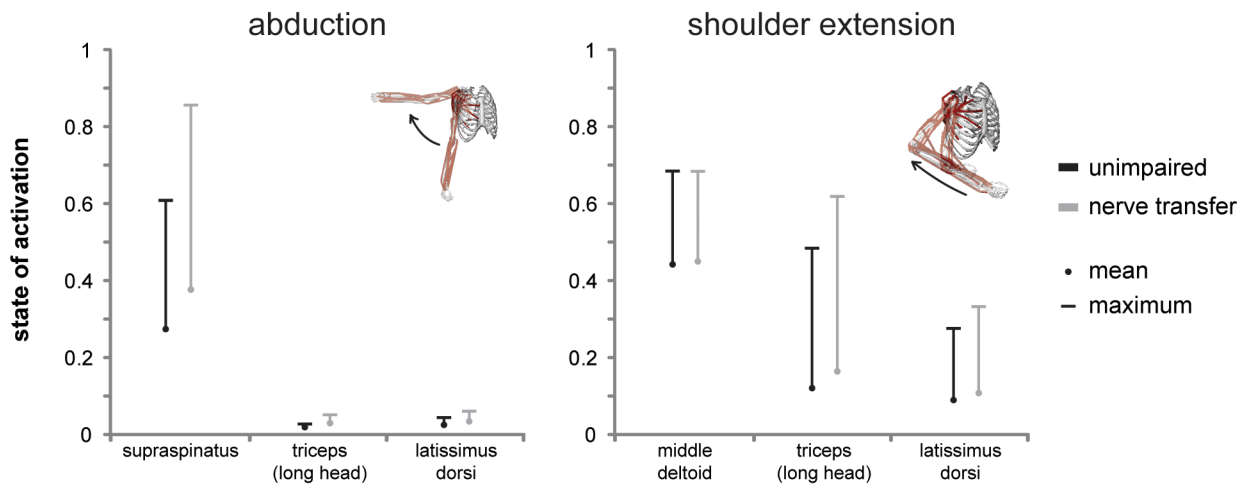


Figure 6. Mean and maximum states of activation of select compensatory muscles during the abduction and shoulder extension movement simulations, both with and without simulated posterior deltoid and teres minor paralysis
Compensatory muscles were not fully activated during movement simulations even when the posterior deltoid and teres minor were paralyzed.